NUMERICAL INVESTIGATION AND COMPARISON OF THE RECTANGULAR, CYLINDRICAL, AND HELICAL-TYPE DC ELECTROMAGNETIC PUMPS

Authors: Lee, G., & Kim, H.R*.

Journal Information:

- **Journal:** Magnetohydrodynamics
- **Year:** 2017
- **Volume:** 53(2)
- **Pages:** 429-438
- **DOI:** https://doi.org/10.22364/mhd.53.2.23

NUMERICAL INVESTIGATION AND COMPARISON OF THE RECTANGULAR, CYLINDRICAL, AND HELICAL-TYPE DC ELECTROMAGNETIC PUMPS

Geun Hyeong Lee, Hee Reyoung Kim*
Ulsan National Institute of Science and Technology, Ulsan 689-798, Republic of Korea

Abstract

Rectangular-, cylindrical-, and helical-type DC electromagnetic pumps with a low flowrate of 6 cc/s and a developed pressure of 10 bar were comparatively analyzed for a liquid lithium transportation system operating at a temperature of 300 °C. The design variables for DC electromagnetic pumps with different types of geometries were optimized to attain the required flowrate and developed pressure. The relation between the developed pressure and the input current was analyzed for an incompressible liquid metal flow in the channels of all three types of DC electromagnetic pumps. Theoretical calculations showed that the helical-type DC electromagnetic pump, which had multiple connected ducts with parallel contacts for a reduced input current, needed 12% of the current of the rectangular- and cylindrical-type pumps in order to satisfy the hydrodynamic conditions, despite the more or less complex geometry.

Keywords: DC Electromagnetic Pumps, Design, Liquid Metal Pumps, Optimization

NOMENCLATURE

B	Magnetic flux density [T]
D	Equivalent hydraulic diameter [m]
D_i	Inner diameter of the pump duct [m]
D_r	Diameter of the overall pump duct [m]
E_p	Electromotive force [V]
f	Force density [N/m^3]
f_d	Darcy friction factor
f_r	Minor friction factor
H_d	Pump duct height, except the wall thickness along the permanent-magnet direction [m]
i_f	Fringe current [A]
i_t	Total input current [A]
i_p	Liquid metal flow current [A]
i_s	Pump wall current vertical to the electrode stub direction [A]
i_{ver}	Current vertical to the electrode stub direction [A]
J_t	Total current density [A/m^2]
J_e	Current density from the electrode stub [A/m^2]
K_1	Loop friction loss factor
K_L	Minor friction loss factor
L	Length of the pump duct [m]
n_t	Number of pump duct connections
n_c	Number of electrode stubs
P	Total developed pressure of pump duct[Pa]
P_h	Hydraulic pressure loss in the pump [Pa]
P_e	Pressure loss due to the electromotive force [Pa]
P_L	Developed pressure of pump duct due to the Lorentz force [Pa]
Q	Flow rate [m^3/s]
R_e	Reynolds number
R_f	Fringe resistance [Ω]
R_o	Outer resistance [Ω]
R_p	Liquid lithium resistance [Ω]
R_s	Pump wall resistance vertical to the electrode stub direction [Ω]
R_{ver}	Resistance vertical to the electrode stub direction [Ω]
v	Mean velocity of the fluid [m/s]
W_d	Pump duct width, except the wall thickness along the electrode stub direction [m]
ε_s	Roughness of the liquid lithium [m]
ρ'	Resistivity of the liquid lithium [Ω · m]
ρ_{lit}	Density of the liquid lithium [kg/m^3]
σ	Electrical conductivity of the material [1/(Ω · m)]

1. Introduction

Electromagnetic pumps have been used for transporting liquid metal having a high electrical conductivity. They have the advantages of no moving and sealing parts, eliminating the possibility of leakage and abrasion compared to mechanical pumps. In particular, DC electromagnetic pumps, which are used for various experimental purposes and have a low flowrate and different developed pressures, have the advantage of geometrical simplicity from a design aspect, even though a relatively high input current is required to transport liquid metal. DC-conduction-type electromagnetic pumps are used to transport liquid lithium for the creation of a thin liquid lithium metal film; for example, a linear accelerator requires the charge elimination of heavy ions by using a charge stripper having the form of the thin liquid metal film. Geometrically, DC-conduction-type electromagnetic pumps are categorized into rectangular, cylindrical, and helical types, as shown in Fig 1. The electromagnetic force is produced in the axial direction at rectangular and cylindrical types and in the azimuthal direction at helical type by the vector product of current density (J) and magnetic field (B), respectively. In the present study, these three types of DC electromagnetic pumps are comparatively investigated with regard to the developed pressure on the input current.

2. Analysis

A DC electromagnetic pump has three major parts: an electrode stub, a permanent magnet, and a pump duct. In Fig. 1, the pressure in the pump channel is developed by the Lorentz force, which is generated by the vector product of the current and the magnetic field. The current density can be expressed using Ohm's law in Eq. (1), and the Lorentz force can be obtained with Eq. (2). The Lorentz force is included as an external term in the momentum equation of the Navier–Stokes equations, as in Eq. (3). Therefore, the developed pressure of the DC electromagnetic pump is analyzed by solving the coupled equations in Eqs. (1)–(3).

$$\vec{J_{\mathrm{t}}} = \vec{J_e} + \sigma\vec{v} \times \vec{B} \tag{1}$$

$$\vec{f} = \vec{J_t} \times \vec{B} \tag{2}$$

$$\frac{\partial\vec{v}}{\partial t} + (\vec{v}\cdot\nabla)\vec{v} = -\frac{1}{\rho'}\nabla(\vec{P} + \vec{P_h}) + \nu\nabla^2\vec{v} + \frac{1}{\rho'}\vec{J_t} \times \vec{B} \tag{3}$$

First, the Lorentz force is expressed as a function of the external current, electrical conductivity, velocity, and magnetic flux density by substituting Eq. (1) into Eq. (2), resulting in

$$\vec{f} = \vec{J_e} \times \vec{B} + \sigma(\vec{v} \times \vec{B}) \times \vec{B} \tag{4}$$

Eq. (3) is reduced to Eq. (5) for a steady-state incompressible liquid lithium flow, where the viscous term is negligible owing to the high Hartmann number of the electromagnetic pump. Therefore, the pressure gradient in the Navier–Stokes equation is expressed as a function of the current density and magnetic flux density:

$$\nabla P = \frac{\vec{J_t}\times\vec{B}}{L} - \nabla P_h \tag{5}$$

The characteristics of the three types of electromagnetic pumps are analyzed by using equivalent electric circuit methods with the MHD information from Eq. (1)–(5).

The electric circuit methods [1] for rectangular- and cylindrical-type DC electromagnetic pumps are presented in Fig. 2. The electromotive force (EMF) and the resistance of the pump duct affect the force produced inside the liquid lithium. An equation for the rectangular-type DC electromagnetic pump is obtained by Kirchhoff's and Ohm's laws to derive the developed pressure in the liquid lithium of the pump channel. From Kirchhoff's law, the vertical component of current flowing in the direction of electrode stub and total input current are represented as

$$\mathrm{i_{ver}} = \mathrm{i_f} + \mathrm{i_s} \tag{6}$$

$$\mathrm{i_t} = \mathrm{i_p} + \mathrm{i_{ver}} \tag{7}$$

The resistance [2] in the direction vertical to the current flow is expressed as

$$\frac{1}{\mathrm{R_{ver}}} = \frac{1}{\mathrm{R_f}} + \frac{1}{\mathrm{R_s}} \tag{8}$$

By applying Ohm's law, the voltage is acquired according to the current path as

$$\mathrm{R_o i_t} + \mathrm{R_{ver} i_{ver}} = \mathrm{R_o i_t} + \mathrm{R_p i_p} + \mathrm{E_p} = \mathrm{V} \tag{9}$$

The EMF interrupts the force generated (Voltage) according to the Lorentz principle, where it is opposite to the generated force (Voltage), as follows:

$$\mathrm{E_p} = \mathrm{BW_d v} \tag{10}$$

The developed pressure is calculated by dividing the Lorentz force, which is the product of the magnetic flux density and current and W_d, by the flow area ($H_d * W_d$) as

$$\Delta\mathrm{P_L} = \frac{\mathrm{B}}{\mathrm{H_d}}\mathrm{i_p} \tag{11}$$

The current flowing in the liquid lithium is obtained by combining Eqs. (7), (9), and (10) and eliminating the outer resistance and vertical current flow as

$$i_p = \frac{R_{ver} i_t - B w_d v}{R_p + R_{ver}} \tag{12}$$

Moreover, the hydraulic pressure drop [3] is calculated by the Darcy–Weisbach formula:

$$\Delta P_h = \frac{f_d \rho L v^2 (W_d + H_d)}{4 W_d H_d} \tag{13}$$

The friction coefficient is expressed as a function of the Reynolds number as

$$f_d = \frac{64}{R_e} \tag{14}$$

$$\frac{1}{\sqrt{f_d}} = -1.8 \log_{10} \left[\frac{6.9}{R_e} + \left(\frac{\varepsilon_s}{3.7D} \right)^{1.11} \right] \tag{15}$$

for laminar and turbulent flow, respectively [5].

The developed pressure and total input current of the rectangular-type DC electromagnetic pump are obtained by subtracting the hydraulic pressure drop in Eq. (13) from Eq. (11) and applying Eq. (12) as follows:

$$\Delta P = \frac{B i_t R_{ver}}{(R_{ver} + R_p) H_d} - \frac{B^2 Q}{(R_{ver} + R_p) H_d^2} - \frac{f_d \rho_{lit} L v^2 (W_d + H_d)}{4 W_d H_d} \tag{16}$$

$$i_t = \left(\Delta P + \frac{B^2 Q}{(R_{ver} + R_p) H_d^2} + \frac{f_d L \rho_{lit} v^2 (W_d + H_d)}{4 W_d H_d} \right) \frac{(R_{ver} + R_p)}{R_{ver}} \frac{H_d}{B} \tag{17}$$

The electric circuit of the cylindrical-type DC electromagnetic pump is the same as that of the rectangular-type pump, as shown in Fig. 2, because the solution method is the same, except for the cylindrical geometry. The developed pressure and total input current of the cylindrical-type DC electromagnetic pump are as follows:

$$\Delta P = \frac{4 B i_t R_{ver}}{\pi (R_{ver} + R_p) D_i} - \frac{16 B^2 Q}{\pi^2 (R_{ver} + R_p) D_i^2} - \frac{f_d \rho_{lit} L v^2}{2 D_i} \tag{18}$$

$$i_t = \left(\Delta P + \frac{16 B^2 Q}{\pi^2 D_i^2 (R_{per} + R_p)} + \frac{f_d \rho_{lit} L v^2}{2 D_i} \right) \frac{(R_{per} + R_p)}{R_{per}} \frac{\pi D_i}{4 B} \tag{19}$$

The electric circuit for the helical-type DC electromagnetic pump has multiple equivalent resistances due to several tubes that compose the pump duct and are connected to the electrode stub, as shown in Fig. 3. The total current flow is divided into multiple flows equal to the number of electrode stubs, and the developed pressure is multiplied by the number of wound pump ducts, which are helically rotated in Fig. 1, and is expressed as

$$\Delta P_L = n_t n_c \frac{4 B i_{per}}{\pi D_i} \tag{20}$$

The helical geometry of the pump duct has an additional term due to the hydraulic pressure drop [4] because of its bent duct shape:

$$\Delta P_{h,minor} = \frac{k_L \rho_{lit} v^2}{2} \tag{21}$$

where

$$k_L = 4 n_t \left(\frac{f_r \pi D_R}{8 D_i} + 0.5 K_1 \right) + K_1 \tag{22}$$

Therefore, the total developed pressure and total input current of the helical-type DC electromagnetic pump are expressed as

$$\Delta P = n_t \left(\frac{4 B i_t R_{ver}}{\pi (R_{ver} + R_p) D_i} - \frac{16 \ c B^2 Q}{\pi^2 (R_{ver} + R_p) D_i^2} \right) - \frac{\pi n_t D_R f_d \rho_{lit} v^2}{2 D_i} - \frac{k_L \rho_{lit} v^2}{2} \tag{23}$$

$$i_t = \left(\Delta P + \frac{16 n_t n_c B^2 Q}{\pi^2 D_i^2 (R_{per} + R_p)} + \frac{\pi f_d \rho_{lit} n_t D_r v^2}{2 D_i} + \frac{k_L \rho_{lit} v^2}{2} \right) \frac{(R_{per} + R_p)}{n_t R_{per}} \frac{\pi D_i}{4 B} \tag{24}$$

3. Results and Discussion

The wall thickness of the rectangular duct type pump duct was 0.001 m in Fig 4. The permanent magnet thickness was restricted as 0.05 m due to machinability limitation. The magnetic flux density was decreased as the height of the pump was increased whereas it had maximum value at the specific width and length of the pump. The input current was proportional to the height of the rectangular pump duct when it was greater than 0.001 m, satisfying the machinability limitations in Fig. 4. Therefore, the width and length of the rectangular pump ducts should be determined to optimize the input current in Fig. 5 and Fig. 6. The optimized input current of the rectangular pump was 2280 A when the width and length of the rectangular pump duct were 0.032m and 0.08 m, respectively.

The wall thickness of the cylindrical pump duct was 0.001 m, which was the same as that of the rectangular pump. The length of the cylindrical pump duct was determined to be 0.05 m owing to the limit of the permissible current to the electrode stub. The input current versus the change in the diameter of the cylindrical pump is shown in Fig. 7, where the input current is proportional to the inner diameter of the cylindrical pump. The minimum allowable size of the inner diameter of the cylindrical pump was restricted to 0.002 m owing to machinability limitations. Therefore, the required input current was 2089 A, which was about 8.4 % lower than that of the rectangular pump, for a developed pressure of 10 bar due to higher magnetic flux density.

The helical pump has a force that multiplies the force at a single tube by the number of bent tubes inside the liquid lithium. Accordingly, the required input current is reduced, which is proportional to the number of turns

of tubes in Fig. 8. The magnetic flux density of the helical pump was higher than those of the other pumps where it was constant as 1 T because ferromagnet induced the magnetic flux path. The wall thickness of the pump duct was 0.001 m, which was the same as that of the rectangular pump. The input current attained its minimum value when the inner diameter of the tube was 0.002 m, resulting in an input current of 204 A. The input current was significantly lower than those of the rectangular and cylindrical pumps, where the maximum number of turns of the tube was limited to 10 considering the space in which the helical pump was to be installed.

The characteristics of the developed pressure and flowrate for the three types of pumps based on variable optimization are shown in Fig. 9. The rectangular- and helical-type pumps were thought to be more stable than the cylindrical-type pump, considering that the slopes were negative at all flowrates. The hydrodynamic, geometrical, and electrical design variables of the three types of electromagnetic pumps are summarized in Tables 1–3. The Lorentz force of the helical-type electromagnetic pump was 10~12 times higher than those of the rectangular- and cylindrical-type pumps for the same input current because of the parallel connection of the pump duct geometry and higher magnetic flux density. However, the pressure loss of the helical-type pump was 14~52 times higher than those of the rectangular- and cylindrical-type pumps. As a result, the input current of the helical-type DC electromagnetic pump was found to be the lowest—about 9 % of the rectangular- and cylindrical-type pumps—for the requirements of a flowrate of 6 cc/s and a developed pressure of 10 bar.

4. Conclusion

A comparison and an optimization analysis of three types of DC electromagnetic pumps with a flow rate of 6 cc/s and a developed pressure of 10 bar were carried out for the transport of liquid lithium for a charge stripper at a temperature of 300 °C. It was thought that the helical-type DC electromagnetic pump could be most effectively used for lithium liquid transport because it has the lowest input current among the three types of DC electromagnetic pumps.

References

[1] B. K. NASHINE, S. K. DASH, K. GURUMURTHY, U. KALE, V. D. SHARMA, R. PRABHAKAR, M. RAJAN, AND G. VAIDYANATHAN. Performance testing of indigenously developed DC conduction pump for sodium cooled fast reactor. *Indian J. Eng. Mater. Sci.*, vol. 14 (2007), pp. 209-214.

[2] R. S. BAKER AND M. J. TESSIER. *Handbook of Electromagnetic Pump Technology* (Elsevier, New York, 1987).

[3] S. J. ZINKLE. Summary of physical properties for lithium, Pb-17Li, and $(LiF)_n \cdot BeF_2$ coolants. In *APEX Study Meeting*, 1998.

[4] CRANE CO. *Flow of Fluids through Valves, Fittings, and Pipe* (Crane Co., Chicago, 1988).

[5] S. E. HAALAND. Simple and explicit formulas for the friction factor in turbulent pipe flow, *J. Fluids Eng.*, vol. 105 (1983), pp. 89-90.

Table captions

Table. 1 Design specifications of the rectangular-type DC electromagnetic pump
Table. 2 Design specifications of the cylindrical-type DC electromagnetic pump
Table. 3 Design specifications of the helical-type DC electromagnetic pump

Table 1

	Design variable	Units	Value
Hydrodynamic	Flow rate (Q)	[m^3/s]	0.000006
	Developed pressure (ΔP)	[bar]	10
	Velocity (v)	[m/s]	0.19
	Reynolds number (R_e)	-	406
	Hydraulic pressure loss (ΔP_h)	[bar]	0.00057
	EMF pressure loss (ΔP_e)	[bar]	0.12
Geometrical	Height (H_d)	[m]	0.001

	Width (W_d)	[m]	0.032
	Length (L)	[m]	0.08
Electrical	Input current (i_t)	[A]	2280
	Magnetic flux density (B)	[T]	0.76

Table 2

	Design variable	Units	Value
Hydrodynamic	Flow rate (Q)	[m^3/s]	0.000006
	Developed pressure (ΔP)	[bar]	10
	Velocity (v)	[m/s]	1.91
	Reynolds number (R_e)	-	4266
	Hydraulic pressure loss (ΔP_h)	[bar]	0.0035
	EMF pressure loss (ΔP_e)	[bar]	0.031
Geometrical	Inner diameter (D_i)	[m]	0.002
	Length (L)	[m]	0.05
Electrical	Input current (i_t)	[A]	2089
	Magnetic flux density (B)	[T]	0.83

Table 3

	Design variable	Units	Value
Hydrodynamic	Flow rate (Q)	[m^3/s]	0.000006
	Developed pressure (ΔP)	[bar]	10
	Velocity (v)	[m/s]	1.91
	Reynolds number (R_e)	-	4266
	Hydraulic pressure loss (ΔP_h)	[bar]	0.38
	EMF pressure loss (ΔP_e)	[bar]	1.36
Geometrical	Inner diameter (D_i)	[m]	0.002
	Overall diameter (D_r)	[m]	0.172
	Number of connections (n_t)	-	10
	Number of electrode stubs (n_c)	-	3
Electrical	Input current (i_t)	[A]	204
	Magnetic flux density (B)	[T]	1

Figure captions

Fig. 1 Schematics of (a) rectangular-, (b) cylindrical-, and (c) helical-type DC electromagnetic pumps
Fig. 2 Electrical equivalent circuit of the rectangular- and cylindrical-type DC electromagnetic pumps
Fig. 3 Electrical equivalent circuit of the helical-type DC electromagnetic pump
Fig. 4 Input current and magnetic flux density on the change of the height in the rectangular-type pump
Fig. 5 Input current and magnetic flux density on the change of the width in the rectangular-type pump
Fig. 6 Input current and magnetic flux density on the change of the length in the rectangular-type pump
Fig. 7 Input current and magnetic flux density on the change of the inner diameter in the cylindrical-type
Fig. 8 Input current on the change of the number of tube turns in the helical-type pump
Fig. 9 Developed pressure–flowrate curves of the three types of DC electromagnetic pumps

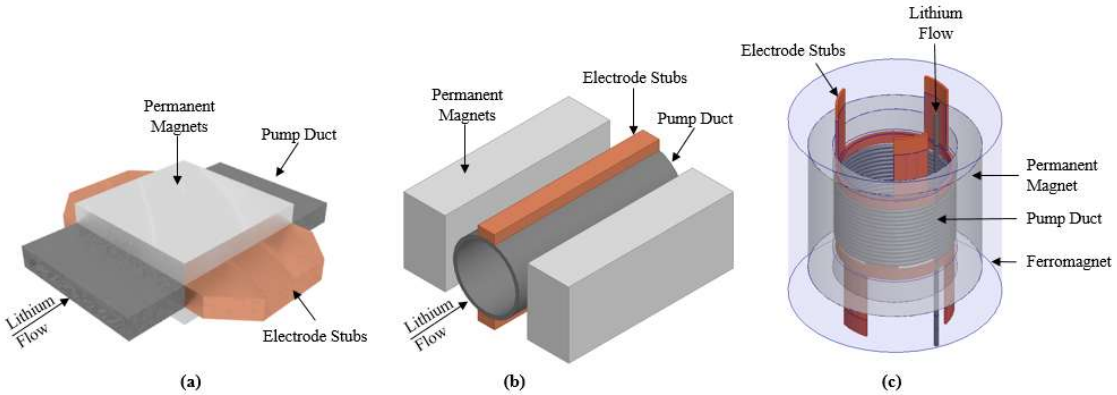

Fig. 1

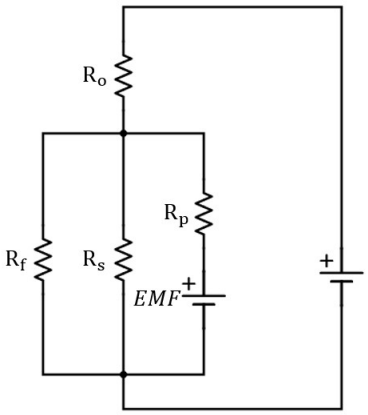

Fig. 2

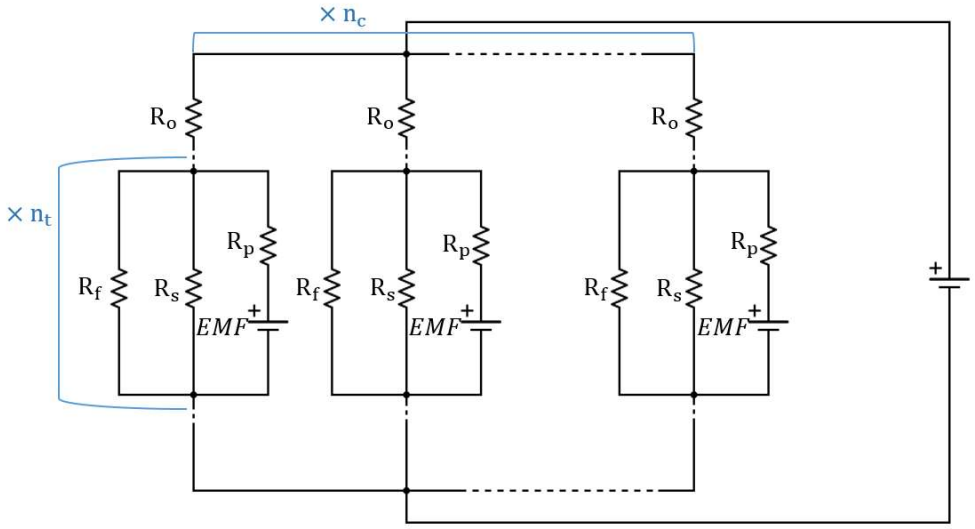

Fig. 3

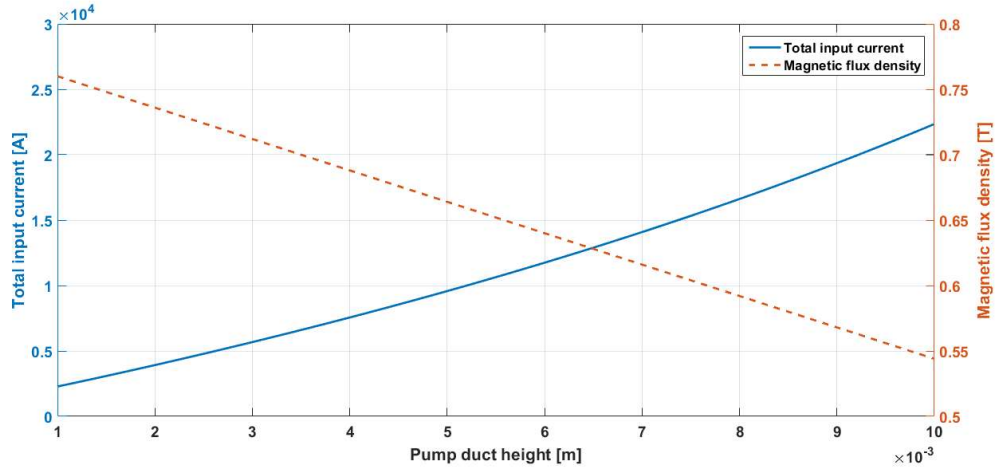

Fig. 4

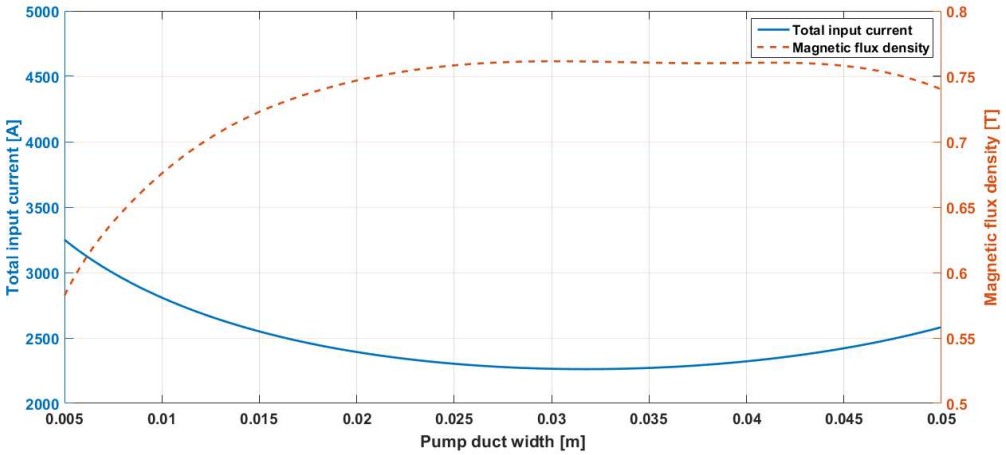

Fig. 5

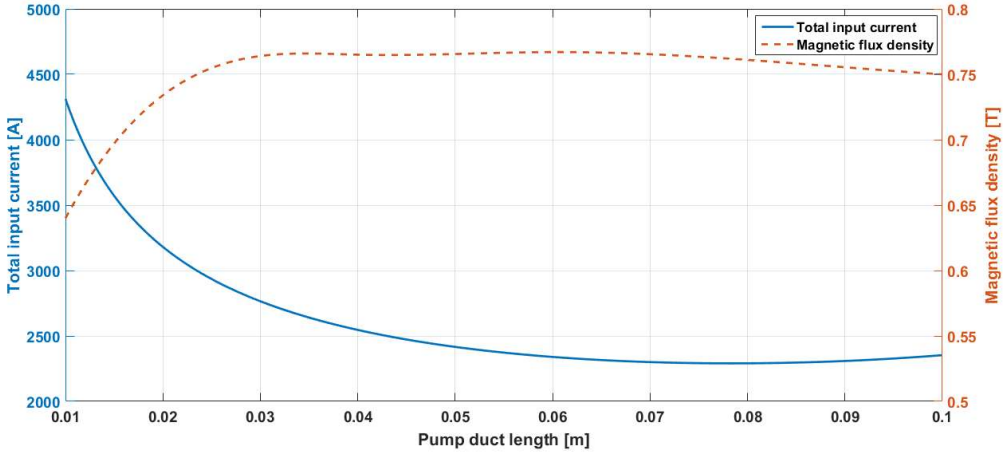

Fig. 6

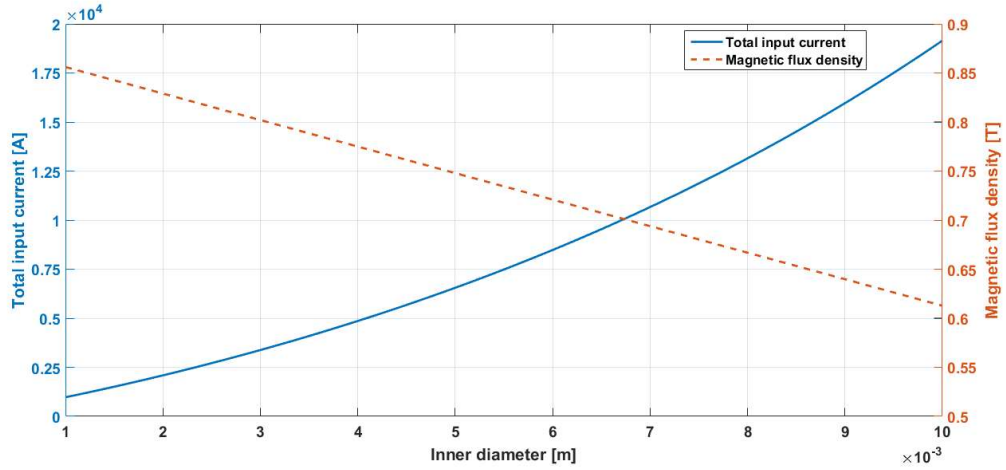

Fig. 7

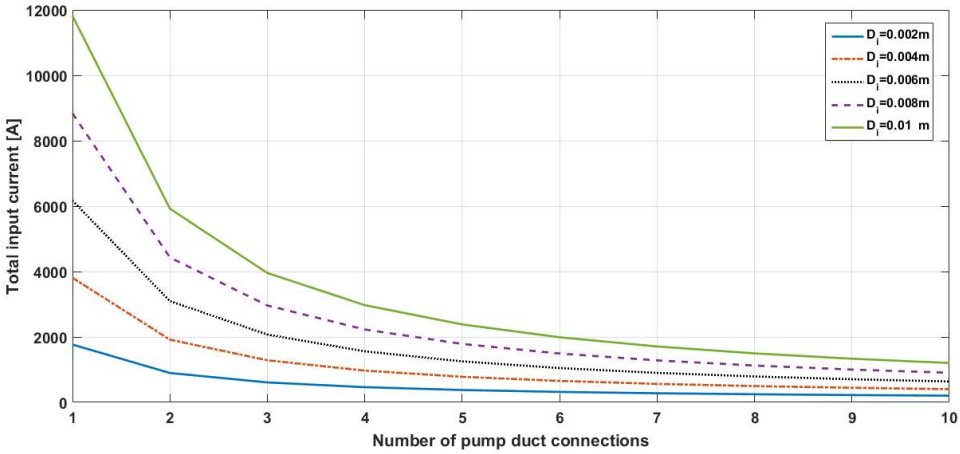

Fig. 8

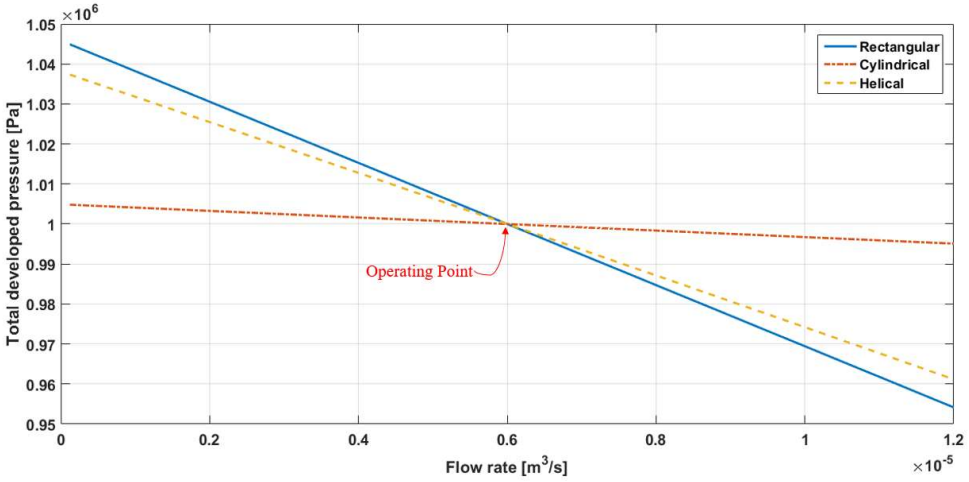
×10^6
1.05
1.04
1.03
1.02
1.01
1
0.99
0.98
0.97
0.96
0.95
Total developed pressure [Pa]
0
0.2
0.4
0.6
0.8
1
1.2
×10^-5
Flow rate [m^3/s]
Rectangular
Cylindrical
Helical
Operating Point

Fig. 9